fractal and fractional

MDPI

Article

Higuchi Fractal Dimension with Fréchet Distance (HFDf) to Assess Cortical Neurodynamics

Karolina Armonaite [1], Alisson Pamela Mallqui Ramirez [2], Lorenza Cicerone [2], Federico Cecconi [3], Angelica Quercia [4], Livio Conti [5,6], Fabiano Bini [2], Franco Marinozzi [2], Luca Paulon [7], Camillo Porcaro [3,8] and Franca Tecchio [3,*]

1 Faculty of Mathematics and Natural Sciences, Kaunas University of Technology, 44249 Kaunas, Lithuania
2 Department of Mechanical and Aerospace Engineering, "Sapienza" University of Rome, 00184 Rome, Italy; mallquiramirez.1514173@studenti.uniroma1.it (A.P.M.R.); cicerone.1948482@studenti.uniroma1.it (L.C.); fabiano.bini@uniroma1.it (F.B.); franco.marinozzi@uniroma1.it (F.M.)
3 Laboratory of Electrophysiology for Translational NeuroScience (LET'S), Institute of Cognitive Sciences and Technologies—Consiglio Nazionale delle Ricerche, 00196 Rome, Italy; camillo.porcaro@unipd.it (C.P.)
4 Department of Neurology and Sleep Research Centre, Oasi Research Institute-IRCCS, 94018 Troina, Italy; aquercia@oasi.en.it
5 Faculty of Engineering, Uninettuno University, 00186 Rome, Italy; livio.conti@uninettunouniversity.net
6 INFN—Istituto Nazionale di Fisica Nucleare, Sezione Roma Tor Vergata, 00133 Rome, Italy
7 Independent Researcher, 00159 Rome, Italy; luca.paulon@gmail.com
8 Biomedical Engineering Research to Advance and Innovate Translational Neuroscience (BRAIN Unit), Department of Neuroscience & Padova Neuroscience Center, University of Padova, 35128 Padova, Italy
* Correspondence: franca.tecchio@cnr.it

Abstract

The temporal course of neuronal electric activity within brain networks, or neurodynamics, reflects the structural and functional properties of the neuronal populations that generate it. Using intracranial stereo-electroencephalography (sEEG) recordings from the public Montreal Neurological Institute (MNI) atlas, we investigated neurodynamics in the primary motor (M1), somatosensory (S1), and auditory (A1) cortices. We tested whether modifying the Higuchi fractal dimension (HFD) by replacing the Euclidean distance with the Fréchet distance could improve sensitivity to local neurodynamics by incorporating trajectory-based similarities in signal evolution. Using a conservative within-subject approach established in the previous literature, we compared signals recorded from different cortical areas within the same individuals (M1 vs. S1: # of people = 16; M1 vs. A1: # = 9; S1 vs. A1: # = 6). To delve deeper into the new measure's meaning, it was tested on sequences with known fractal properties, the Brownian motion and the Weierstrass function. Results showed that the newly introduced Fréchet-based HFD (HFDf), similarly to standard HFD, consistently discriminated cortical areas at the intra-subject level, confirming the robustness of fractal dimension as a descriptor of region-specific neurodynamics. Contrary to our hypothesis, HFDf did not provide additional sensitivity across areas and notably, it displayed less evident reduction of values in sleep than awake. While cortical regions may share common governing principles across spatiotemporal scales, these do not necessarily translate into strict similarity in temporal signal morphology. We suggest that these findings support that the free-scale nature of neurodynamics is not a self-similar one. This refinement of quantitative tools for cortical neurodynamic mapping paves the way towards novel tools for neuroimaging-informed neuromodulation strategies.

Keywords: complexity; neurodynamics; stereo-electroencephalography (sEEG); Fréchet distance; morphology; structure–function unit; feedback–synchrony–plasticity (FeeSyCy)

Academic Editor: Christoph Bandt

Received: 2 May 2026
Revised: 24 June 2026
Accepted: 29 June 2026
Published: 6 July 2026

1. Introduction

1.1. Scale-Free Neurodynamics

Scale-free properties have been reported across brain activity and behavior, suggesting that neural dynamics are organized over multiple temporal and spatial scales rather than around a single characteristic scale [1]. Seminal studies proposed neuronal avalanches as a general property of cortical networks, supporting efficient information transmission while maintaining network stability [2]. Subsequent investigations showed that brain activity exhibits scale-free temporal organization with characteristics that differ from those observed in other natural systems, suggesting specific underlying generative mechanisms [3]. Consistently, network topology and hierarchical recruitment of neuronal populations have been proposed as key contributors to the emergence of multiscale dynamics and synchronization properties in cortical networks [4]. Within this framework, the concepts of scale-free organization, fractality, and self-similarity have often been discussed in close association, and in some cases used interchangeably [5].

1.2. Neurodynamics as a Signature of Cortical Areas

The temporal evolution of neuronal electrical activity—here referred to as neurodynamics [6–8]—reflects the structural and functional organization of the neuronal pools that generate it. In other words, beyond amplitude or spectral content, the shape of neural activity over time emerges as a result of local and distributed circuit interactions and feedback integration, and expresses functional specialization. These findings indicate that ongoing neuronal activity exhibits region-specific temporal patterns that remain recognizable across individuals and behavioral states [9]. These patterns have been interpreted as signatures of cortical areas, rooted in their specific cytoarchitecture, connectivity, and position within large-scale networks.

1.3. From Morphology of Evoked Responses to Resting-State Dynamic Patterns

Sensory perception relies on an anatomical hierarchy of neural networks composed of synaptic relays recruited through predominantly feed-forward information flow, continuously modulated by inter-nodal feedback. When a stimulus activates such a circuit, the resulting neuronal response does not merely vary in amplitude or latency, but assumes a dynamic temporal shape that reflects both the underlying anatomy and the sequence of neuronal recruitment. Accordingly, the morphology of evoked responses is systematically specific to sensory systems: visual, auditory, and somatosensory evoked responses display clearly distinct temporal shapes, mirroring the structural and functional organization of the circuits involved. Within the same sensory system, responses arising from commonly innervated structures exhibit similar morphologies [10]. Notably, homologous networks in the two hemispheres show a remarkable inter-hemispheric similarity of evoked morphology despite inter-subject variability of the overall morphology [10,11]. Such similarities indicate that response morphology retains the imprint of the individual connectivity pattern and the structural architecture of the generating neuronal pools.

These observations support a central concept: the activation of a neuronal circuit gives rise to a temporal form that carries information about both the anatomy and the dynamics of recruitment of the structures involved. This insight provides a natural bridge toward the study of ongoing, resting-state activity, where no external stimulus is present, yet intrinsic circuits continuously self-organize and interact, generating complex dynamic patterns. Along this line, we have shown that functional homology—crucial for learning and adaptive processes—can be explored in the resting state by quantifying the similarity of local neurodynamic patterns. Notably, these neurodynamic similarities are sensitive to hemispheric dominance and exhibit age-dependent modulation [12], suggesting that ongo-

ing resting-state activity of neuronal pools unfolds into nonstationary, complex temporal patterns that relate to functional abilities mediated by intracortical local, long-range, and inter-area connectivity.

1.4. FeeSyCy at Multiple Scales: Fractal Nature of the Local Neurodynamics

The large repertoire of spatiotemporal activity patterns subtending adaptive behavior is suggested to emerge from universal mechanisms of emergent complex phenomena evident in dynamical systems poised near a critical point [13]. In the somatosensory cortex of the newborn rat, spatially confined spindle bursts represent the first and only organized network pattern. The localized spindles are selectively triggered in a somatotopic manner by spontaneous muscle twitches, motor patterns analogous to human fetal movements, indicating that the interaction between movement-triggered sensory feedback signals and self-organized spindle oscillations shapes the formation of cortical connections required for sensorimotor coordination [14].

Neurodynamics unfolds across multiple temporal scales, a property that naturally lends itself to fractal descriptions. Fractal measures capture how neuronal signals incorporate temporal structures whose evolving shapes reflect the underlying cytoarchitecture and connectivity architecture across scales, providing a compact representation of multiscale organization. Among these measures, the Higuchi fractal dimension (HFD) has been widely used to quantify the complexity of electrophysiological signals in both evoked and resting-state activity [15,16].

We introduce here a guiding hypothesis—conceptual rather than directly testable within the present study—that the fractal nature of ongoing local neurodynamics emerges from the persistence of the feedback–synchrony–plasticity (FeeSyCy) principle governing network functioning across multiple organizational levels [7]. This principle operates when network nodes correspond to single neurons, local neuronal populations, cortical areas, or even entire brain–body systems. Within this framework, neurodynamic complexity is expected to relate to network topology: nodes that act as hubs within connectivity architectures may express richer, more multiscale temporal dynamics than peripheral (spoke) nodes. Such a relationship would be consistent with higher fractal dimensions associated with signals generated by more integrative and feedback-rich network counterparts, provided that fractality is estimated using metrics sensitive to temporal pattern morphology.

However, standard implementations of HFD rely on Euclidean distance, which is sensitive to pointwise fluctuations but largely blind to the morphological similarity of temporal patterns. This limits its ability to capture dynamic shapes that arise from coordinated neuronal communication, and motivates the integration of morphology-sensitive metrics, such as the Fréchet distance, into fractal dimension estimation.

1.5. Fréchet Distance as a Morphology-Sensitive Metric

The Fréchet distance offers a complementary approach, as it quantifies the similarity between curves while preserving their temporal ordering [17,18]. Unlike pointwise distances, it is sensitive to the overall shape and progression of signals, making it particularly suitable for comparing neurodynamic features [19].

This computational strategy has proven especially advantageous in navigation systems, where comparing entire trajectories of candidate paths within road networks is critical. In this context, Fréchet-based measures enabled more efficient matching with improved quality and reduced computational cost compared to pointwise approaches [20]. Beyond navigation, the Fréchet distance has demonstrated its ability to capture biologically meaningful patterning, supporting the analysis and retrieval of online handwritten text [21], and the identification of distinct foraging clusters associated with specific bathymetric

features in movement ecology [22]. More generally, the intrinsic ability of the Fréchet distance to quantify ongoing temporal patterning is reflected in its widespread adoption in audio analysis, where it has recently been formalized as a domain-specific metric to characterize perceptual similarity between complex sound signals ("Fréchet Audio distance") [23]. Together, these applications highlight the suitability of the Fréchet distance for contexts in which the morphology and temporal evolution of signals—rather than pointwise similarity—are key to meaningful comparison.

The use of Fréchet distance in neurophysiology has shown that morphology-based comparisons can enhance sensitivity to alterations in dynamic circuit recruitment, for example, those induced by blood flow reduction during middle cerebral artery aneurysm clipping [24]. Integrating Fréchet distance into fractal analysis may therefore enhance the sensitivity of complexity measures to region-specific neurodynamics. The resulting measure, referred to as HFDf, integrates multiscale complexity with morphology-sensitive comparison of temporal patterns. In other words, we maintain the scaling law concept, modifying only the metric.

1.6. Aim: Testing HFDf Sensitivity to Region-Specific Neurodynamics

Unlike spectral approaches based on sinusoidal decomposition and power-law estimation in the frequency domain, the present work aims to characterize neurodynamics directly in the temporal domain, focusing on the multiscale evolution of neuronal activity trajectories. We hypothesize that such an approach may better capture physiologically meaningful aspects of local neurodynamics. Notably, entropy-derived measures have shown limited sensitivity in differentiating cortical regions, whereas fractal approaches consistently revealed region-specific temporal organization. Our goal here is not to introduce a new fractal measure, but rather to explore whether a metric can be simultaneously sensitive to both the assumed scale-free structure of brain signals and the morphology of neurodynamic trajectories, allowing them to be distinguished at the population level. Along this line, we test the hypothesis that the Higuchi fractal dimension (HFD) [25], when computed by replacing the Euclidean distance with the Fréchet distance (HFDf), differs across cortical regions. To maintain continuity with previous studies [26,27], we investigate whether HFDf can discriminate the neurodynamics of the primary motor (M1), somatosensory (S1), and auditory (A1) cortices using intracranial sEEG recordings (Figure 1).

In fact, we highly valued the dataset of primary cortices' representatives derived from the MNI dataset and ready to be interrogated with the present novel approach to regional neurodynamics [26].

Previous evidence indicates that local neurodynamics differs reliably within subjects, with higher-order hubs expressing signals characterized by higher fractal dimension across behavioral states [9] and along the physiological wake–sleep cycle [27]. However, this intra-subject inter-area specificity has so far been outweighed by substantial inter-subject variability, limiting the extension of these markers to population-level inference.

Here, we aim to test whether the introduction of a morphology-sensitive metric into fractal dimension estimation enables a qualitative step forward: namely, whether HFDf can preserve the expected dependence on network role intra-subjectively while also revealing consistent inter-subject differences across cortical regions at the population level.

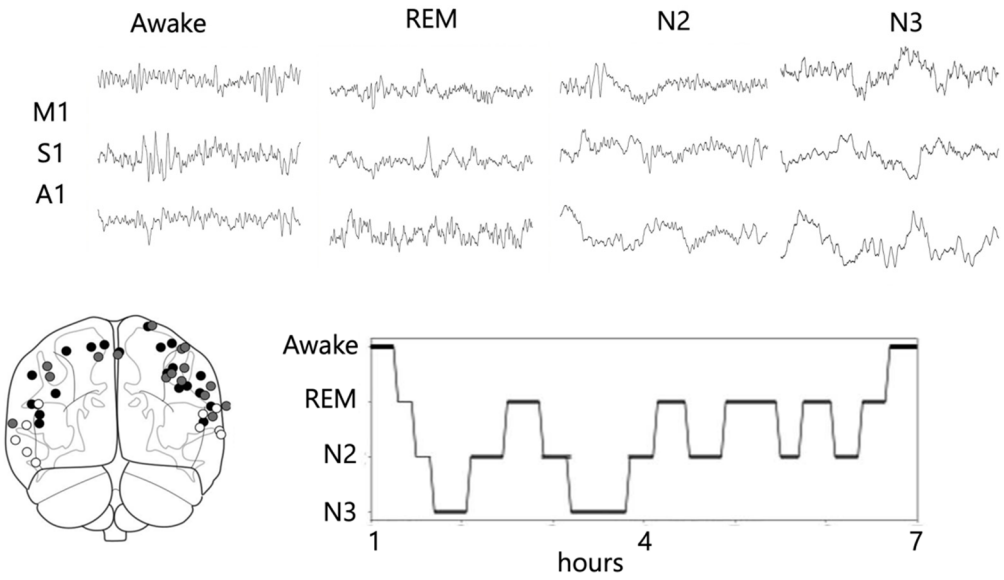

Figure 1. sEEG data from MNI dataset. (**Top**) In one subject, sEEG time course (2 s) of M1, S1, and A1 cortical regions, in the awake and the three studied sleep stages. The amplitude of sEEG in each area is normalized to [−1, 1]. (**Bottom**) Selected channel positions represented in the coronal projection of the subjects having data collected in at least two cortical regions among A1 (white), S1 (gray), and M1 (black). On the right side, a typical hypnogram over the course of a night (figure adapted from [27]).

2. Materials and Methods

2.1. Neurodynamic Data Investigated

We analyzed intracranial stereo-electroencephalography (sEEG) recordings from the publicly available Montreal Neurological Institute (MNI) atlas [28], available at https://mni-open-ieegatlas.research.mcgill.ca/main.php (accessed on 1 February 2021).

The dataset consists of sEEG recordings acquired during eyes-closed resting state from 106 patients (13–68 years, 48 females) diagnosed with refractory focal epilepsy [28,29]. Recordings from areas spared from epileptic alterations were typically obtained using Dixi electrodes, sensitive to neural activity within approximately 2 mm of cerebral tissue. The dataset includes artifact-free signals sampled at 200 Hz, each 1 min long and subdivided into segments of at least 5 s.

As a starting investigation, we adopted a conservative selection strategy to maintain continuity with previous HFD-based assessments sensitive to true intra-subject inter-area neurodynamic relationships. To this end, only subjects with recordings available in at least two cortical regions of interest were included, namely S1-M1, A1-S1, or A1-M1. The available sEEG recordings within primary cortical areas comprised 50 channels for S1, 99 for M1, and 18 for A1. For some subjects, only a single channel was available within a given region of interest, whereas others presented multiple channels in the same area. To ensure homogeneous weighting across subjects, we selected a single representative channel per cortical region for each subject. Channel selection was primarily based on anatomical localization using the spatial coordinates provided in the MNI dataset. For M1 and S1, representative channels were selected so as to correspond to homologous body-part representations. Operationally, we selected M1 and S1 channels with minimal differences in the z coordinate (axial plane) and x coordinate (coronal plane), with M1 channels located more anteriorly (higher y values) than S1 channels along the sagittal plane. For A1, the representative channel was selected as the one located closest to the geometric center among the available channels within the auditory cortex. We include a table with relevant information about the channels in the Supplementary Materials (see Table S1).

2.2. Higuchi Fractal Dimension

HFDf, introduced in this work, modifies the Higuchi fractal dimension by replacing the Euclidean distance with the Fréchet distance. HFD was computed on the same dataset, subjects, and selection criteria in [26] using the procedure recalled below, which provides the reference framework for understanding the modification applied here. For each sEEG channel, the Higuchi algorithm is applied in the time domain by constructing multiple time series through down-sampling the original signal $X(i)$ (with $i = 1, \ldots, N$) every k samples:

$$X_m^k = \{X(m), X(m+k), X(m+2k), \ldots, X(m+int\frac{(N-m)}{k}k)\}, \quad (1)$$

where k is a constant integer value ($2 \leq k \leq$ Kmax) with Kmax < $N/2$ and $m = 2, 3, \ldots, k$. Note that for consistency with HFDf, k started with value 2 to have at least two curves for the Fréchet distance estimate.

To quantify the fractal dimension, HFD calculates the curve length, $L_m(k)$, for each of the k down-sampled curves X_m^k, to assess how these lengths change with the down-sampling factor k.

For each m, the $L_m(k)$ mean Euclidean distance between successive points is calculated:

$$L_m(k) = \left(\sum_{i=1}^{int(\frac{N-m}{k})} |X(m+ik) - X(m+(i-1)k)|\right) \frac{N-1}{int\left(\frac{N-m}{k}\right)k}, \quad (2)$$

Then, HFD considers the average length $L(k)$ obtained by averaging the lengths $L_m(k)$ of the k sub-sequences:

$$L(k) = \frac{1}{k-1} \sum_{m=2}^{k} L_m(k) \quad (3)$$

and finally, HFD is estimated as the slope of the $\log(L(k))$ as a function $\log(1/k)$:

$$\text{HFD} = slope\left(\log(L(k)) \; vs \; \log\left(\frac{1}{k}\right)\right) \quad (4)$$

2.3. Integration of Fréchet Distance Within HFD Estimation

Fréchet distance is defined as the minimum leash length sufficient to join a point traveling forward along one of the curves and one traveling forward along the second curve [30], with the rate of travel for either point not necessarily being uniform, and can be defined as follows.

Given two curves $f, g : [0,\ 1] \rightarrow \mathbb{R}^n$, the Fréchet distance is:

$$d_F(f,g) = inf_{\alpha,\ \beta} max_{t\in[0,1]} \|f(\alpha(t)) - g(\beta(t))\|$$

α and β are continuous, non-decreasing reparametrizations of [0, 1] with $\alpha(0) = \beta(0) = 0$, $\alpha(1) = \beta(1) = 1$. Fréchet distance is zero if the two curves are equal and grows positively as the curves become more dissimilar.

As mentioned above, when replacing the Euclidean distance used in the standard Higuchi algorithm with the Fréchet distance, we compare the shapes of two curves. After a preliminary test phase, we decided to compare each sub-sampled trace with the initial one (Figure 2).

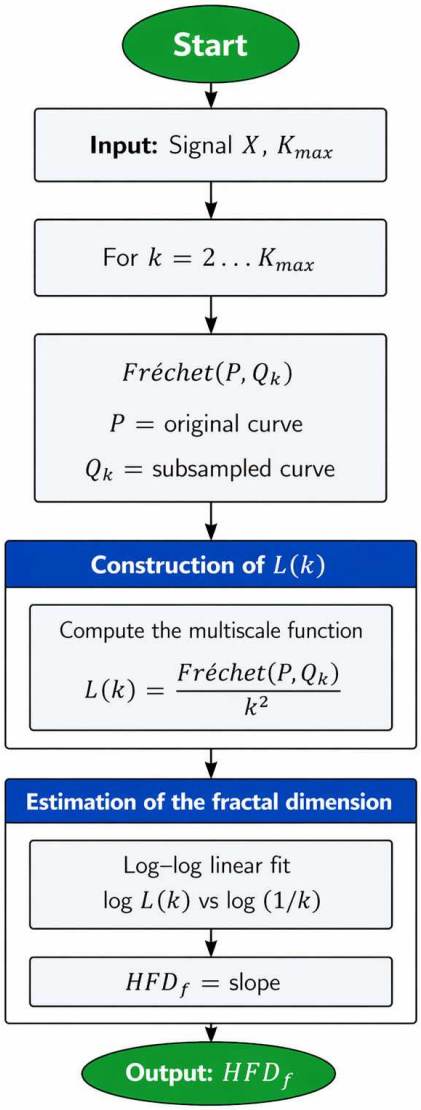

Figure 2. HFDf estimate flowchart. Starting from the original sEEG signal, sub-sampled traces are generated at increasing values of the down-sampling factor k (with $2 \leq k \leq$ Kmax). For each k, the Fréchet distance is computed between the sub-sampled trace and the full original trace used as reference. HFDf is then estimated as the slope of $\log(L(k))$ versus $\log(1/k)$, replacing the Euclidean curve length with the Fréchet-based distance. Code and pseudocode can be found at https://github.com/cecconifederico/HDFf_tool (accessed on 10 June 2026).

As a preliminary assessment to elucidate features of the newly introduced HFDf, Brownian motion sequences and Weierstrass curves with theoretically known fractal dimensions were used to assess the scaling behavior and numerical stability of HFDf estimates.

2.4. Statistical Comparison Across Cortical Areas

We observed that HFDf values, across different sleep stages, show a non-Gaussian distribution (as confirmed by the Shapiro–Wilk test). Thus, in order to compare HFDf values across cortical regions, we used the non-parametric Wilcoxon test (hereafter Wtest values).

HFDf values were compared across cortical regions within subjects to assess whether region-specific neurodynamic signatures can be detected.

3. Results

3.1. Behavior of HFD with Fréchet Distance for Known Curves

To observe the behavior of the new measure for curves with known values of fractal dimension, we selected two cases: Brownian motion as a non-self-similar example and the Weierstrass curve for a self-similar example. Brownian motion can be approximated by a random walk obtained as the cumulative sum of independent Gaussian increments. For a time step Δt, the discrete process is defined as:

$$B_n = \sum_{k=1}^{n} \sqrt{\Delta t}\, \varepsilon_k$$

where $\varepsilon_k \sim N(0,1)$. As $\Delta t \to 0$, the corresponding continuous-time process converges in distribution to Brownian motion $B(t)$. To generate the Weierstrass curve we used a standard definition:

$$W(x) = \sum_{m=0}^{M} a^m cos(b^m \pi x),$$

where $0 < a < 1, b > 1$, $ab > 1$ and we selected $a = 0.5$ and $b = 5$. To have an idea of the stability of the estimate, we generated 10 random sequences of the same length as the sEEG data (12.000 points). Obtained values of HFDf of those sequences are shown in Figure 3.

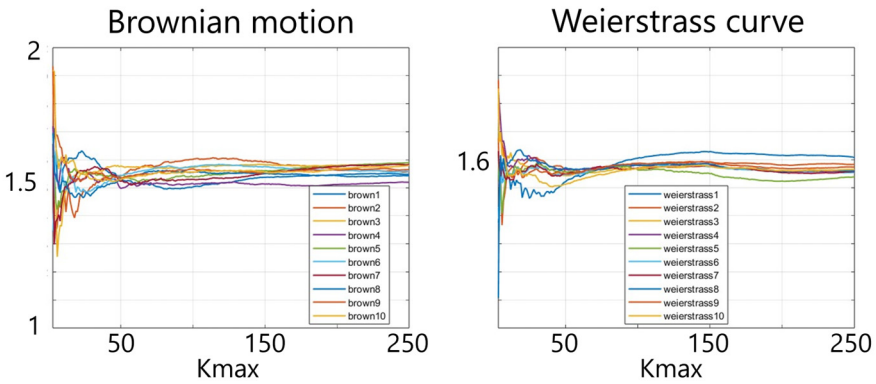

Figure 3. HFDf(Kmax) for 10 synthetically generated Brownian motion and Weierstrass curve sequences.

3.2. Behavior of HFD with Fréchet Distance as a Function of Kmax

We observed stability of the HFDf values in the three cortical regions for the selected Kmax (see Figure 4).

It is worth comparing the dependence on Kmax of the Higuchi fractal dimension computed using the Euclidean distance (HFD, as in [26,27]) with that computed using the Fréchet distance (HFDf, this work), in both cases using the same data, subjects, and selection criteria. We note that HFD does not reach a horizontal asymptote, approaching instead, for high values of Kmax, the upper bound of 2. This issue has been reported in previous studies, where specific selection criteria for Kmax were proposed [26]. In contrast, HFDf exhibits early saturation at about 1.8 (Figure 4).

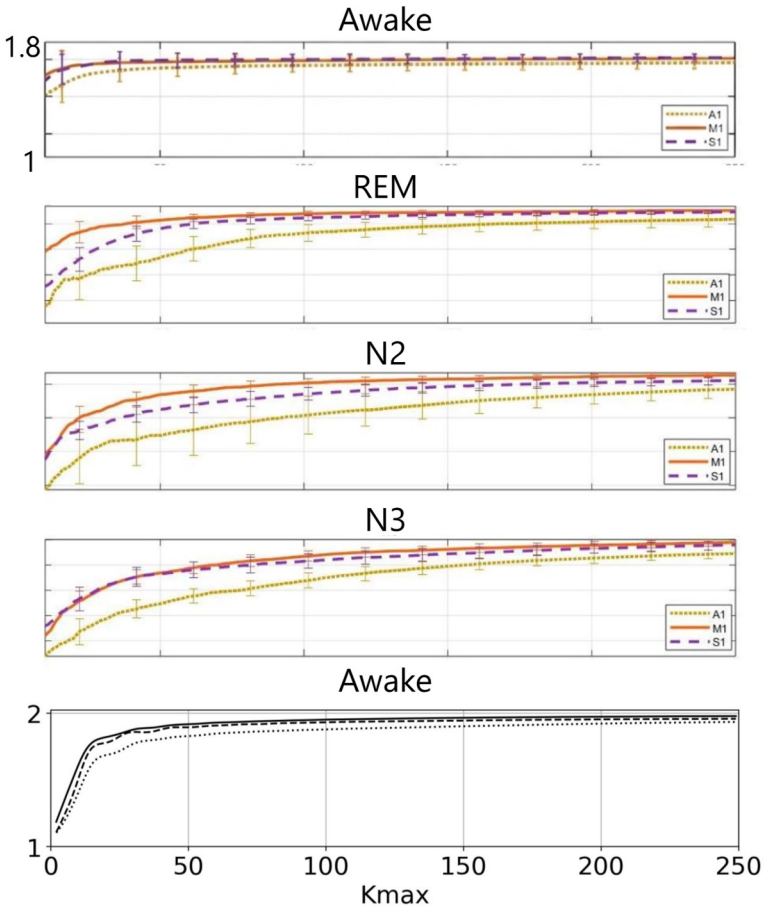

Figure 4. Dependence of HFDf as a function of Kmax. The average of HFDf across all available channels is presented in each of the wake/sleep stages separately, for the three cortical regions. The stability of the relative position of the curves, independently of Kmax, in the three cortical areas is evident. For comparison, we report -in black and white- the behavior of classical HFD in the awake stage for a subset of the same curves, where dotted, dashed and continuous lines represent A1, S1 and M1, respectively.

3.3. Differentiation of HFDf Across Cortical Areas

Median values and interquartile ranges were highly overlapping across regions, reflecting the substantial inter-subject variability already reported for HFD (Table 1). Nevertheless, within-subject comparisons revealed a consistent regional ordering, with M1 generally showing higher HFDf values than S1, and both exceeding A1 across sleep stages (Figure 5, Tables 2 and 3). Both M1 and S1 showed higher HFDf than A1 (Figure 5, Tables 2 and 3).

Table 1. HFDf values.

	Awake			**REM**			**N2**			**N3**		
	M	**IQR**	**#**	**M**	**IQR**	**#**	**M**	**IQR**	**#**	**M**	**IQR**	**#**
M1	1.84	0.09	20	1.80	0.08	13	1.76	0.18	16	1.63	0.18	16
S1	1.84	0.07	17	1.79	0.13	11	1.71	0.14	14	1.62	0.20	14
A1	1.81	0.12	10	1.67	0.16	5	1.66	0.06	6	1.53	0.13	6

Median value (M), interquartile ranges (IQR) and number of people (#) of HFDf in the three cortical regions during wakefulness and sleep.

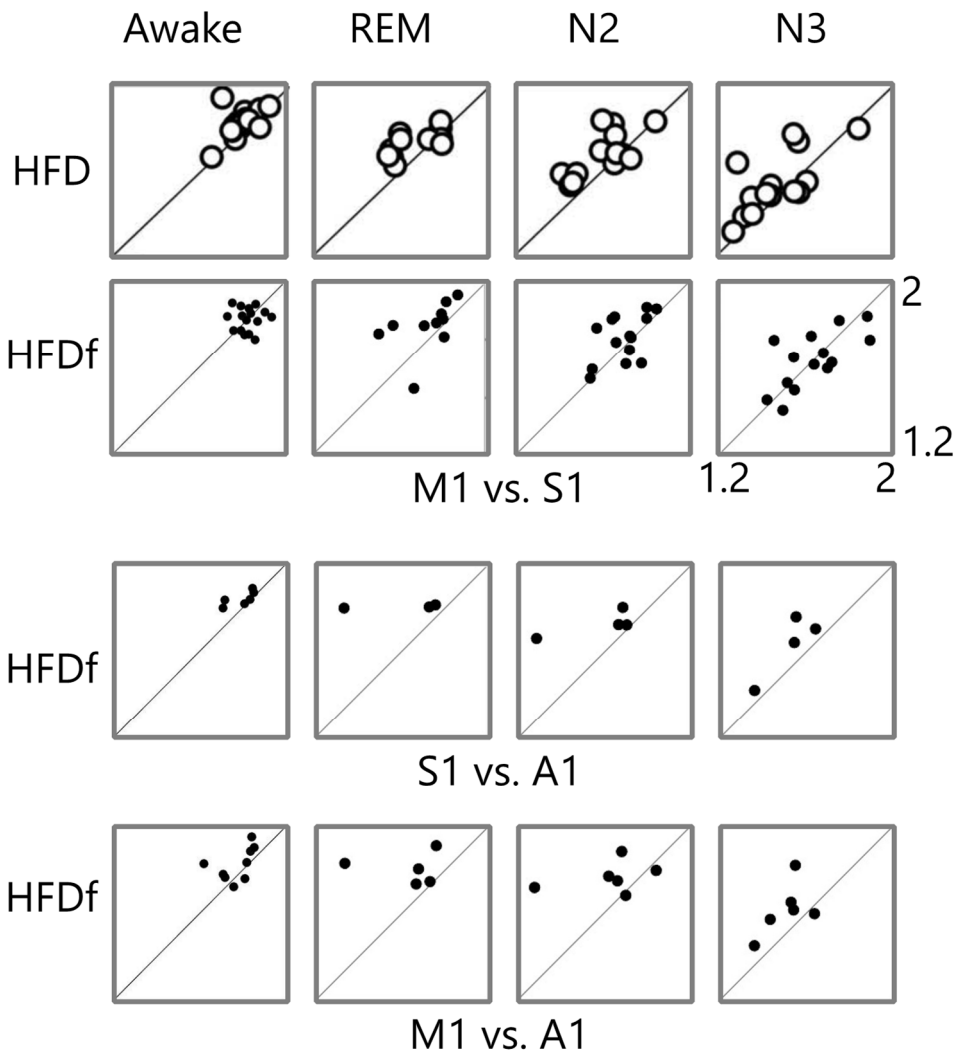

Figure 5. Scatterplot of the HFDf for each pair of cortical regions (on x: S1 in the first and second rows; A1 in the third and fourth; on y: M1 in the first, second and fourth rows, S1 in the third), where each point represents a single subject, across the awake condition and the three sleep stages (REM, N2, N3). Kmax = 35 in all cases. The x- and y-axis scales are equal and range from 1.2 to 2. For direct comparison HFD estimated in [27] is reported for M1 and S1 comparison.

Table 2. Statistics comparing the three cortical regions.

		Awake		**REM**		**N2**		**N3**	
		p	**#**	***p***	**#**	***p***	**#**	***p***	**#**
M1 > S1	HFDf	0.91	16	0.05	11	0.06	14	>0.2	14
	HFD	*0.00*		*0.02*		*0.02*		*0.07*	
M1 > A1	HFDf	0.06	9	0.03	5	0.08	6	0.03	6
	HFD	*0.00*		*>0.2*		*0.08*		*>0.2*	
S1 > A1	HFDf	0.02	6	0.13	3	0.06	4	0.06	4
	HFD	*0.00*		*0.10*		*0.10*		*0.03*	

Statistical significance of Wilcoxon test (*p* value), and number of subjects (#) comparing each pair of regions in the awake stage and the different sleep stages. For direct comparison, the values obtained for HFD in [26,27] are reported in italics.

Table 3. Statistics comparing the awake stage and the different sleep stages.

		M1		S1		A1	
		p	N	*p*	N	*p*	N
Awake > REM	HFDf	>0.2	13	0.03	11	0.06	5
	HFD	*0.00*		*0.01*		*0.21*	
REM > N2	HFDf	0.01	13	0.02	11	>0.2	5
	HFD	*0.00*		*0.02*		*0.21*	
N2 > N3	HFDf	0.00	16	0.04	14	0.04	6
	HFD	*0.00*		*0.00*		*0.08*	

Statistical significance of Wilcoxon test (*p* value), and number of subjects (N) comparing each pair of the awake stage and the different sleep stages for the three cortical regions. For direct comparison, the values obtained for HFD in [26,27] are reported in italics.

The Wilcoxon test applied comparing each pair of cortical regions indicated the relationships described in Table 2. In the comparison between S1 and A1 in REM sleep, given the small sample size of just three subjects, the comparison has limited statistical significance.

We investigated the behavior of HFDf when people were in the awake stage or the different sleep stages and as indicated in Table 3 the general reduction in complexity was not observed for M1 in REM with respect to the awake state. In Tables 4 and 5 the effect sizes are reported as estimated for non-parametric data calculated as the absolute value of Z divided by the square root of the number of observations ($r = |Z| / \sqrt{n}$), where Z represents the standardized Wilcoxon test statistic [31].

Table 4. Effect sizes of the difference between cortical regions.

	Awake		REM		N2		N3	
	r	N	r	N	r	N	r	N
M1 > S1	0.02	16	0.49	11	0.41	14	0.05	14
M1 > A1	0.61	9	0.84	5	0.59	6	0.77	6
S1 > A1	0.89	6	0.77	3	0.82	4	0.82	4

R and number of subjects (N) comparing each pair of regions in the awake stage and the different sleep stages.

Table 5. Effect sizes of the difference between sleep stages.

		M1		S1		A1	
		r	N	r	N	r	N
Awake > REM	HFDf	0.47	13	0.55	11	0.68	5
REM > N2	HFDf	0.68	13	0.61	11	0.21	5
N2 > N3	HFDf	0.86	16	0.45	14	0.68	6

r and number of subjects (N) comparing each pair of sleep stages for the three regions.

4. Discussion

4.1. What Our Data Confirm

In line with the previous literature, fractal dimension proved to be a robust descriptor of local neurodynamics, consistently discriminating cortical areas at the intra-subject level. This confirms that multiscale temporal organization captures relevant aspects of region-specific neuronal activity, as assessed by fractal dimension [15].

The present findings support the view that neurodynamic patterns, i.e., the temporal morphology of neuronal activity, reflect the structural organization of the underlying neuronal pools. In this framework, the temporal evolution of neural signals can be interpreted as a functional expression of circuit architecture, providing a measurable signature of cortical organization.

Nevertheless, a direct comparison between HFD and HFDf behaviors suggests a novelty. As above described, HFD appears sensitive to the richness of multiscale fluctuations, whereas HFDf tends to privilege trajectory morphology. During sleep, neurodynamics undergoes profound reconfiguration rather than a simple reduction in activity, and forcing comparisons toward global morphological similarity may obscure the physiological reduction in complexity observed with conventional HFD.

4.2. What Our Results Do Not Observe

Contrary to our initial hypothesis, incorporating a morphology-sensitive metric through the Fréchet distance (HFDf) did not improve discrimination across cortical areas at population level. The expected gain in sensitivity, based on the ability of the Fréchet distance to capture trajectory similarity, was not observed.

We note that replacing the Euclidean distance with the Fréchet distance shifts the computation from a pointwise comparison along the same trace to a curve-to-curve distance between trajectories. To enable this comparison, we set k = 2, ensuring at least two curves are available (for k = 1 we have the initial curve, with Fréchet distance 0).

A possible interpretation is that neurodynamic patterns reflect structural organization in a scale-dependent manner: similarity of morphology is preserved within comparable structures (e.g., homologous areas [10]), but not across systems operating at different spatial and functional scales. Accordingly, the Fréchet distance, which emphasizes global trajectory similarity, may not capture the specific local temporal features that underpin regional differentiation. Rather, it may impose a form of similarity that is meaningful for homologous or functionally aligned systems, but inconsistent with heterogeneous scales communicating cerebral structures.

4.3. What Do We Learn from Negative Result

The effectiveness of the fractal dimension in capturing regional neurodynamics is consistent with the multiscale organization of brain activity. Neural signals exhibit non-stationary and nonlinear dynamics, with temporal structures distributed across scales, reflecting the interplay of excitation–inhibition balance and network topology [32–34].

A further observation emerged when comparing wakefulness and sleep. Previous studies based on conventional HFD consistently showed a reduction in complexity with increasing sleep depth [27], a finding that [35] exploited, using the fractal dimensions as sensitive markers of shifting dynamics across sleep stages. Partially in contrast, HFDf did not always preserve this modulation. Sleep is not simply associated with a reduction in neuronal activity, but with a profound reconfiguration of thalamocortical and corticocortical interactions [36–38]. This transition manifests as distinct architectural shifts across sleep stages: NREM sleep is characterized by a progressive transition from global integration to segregated modular clusters, whereas REM sleep facilitates a reconfiguration of functional connectivity that creates network patterns distinct from both NREM and wakefulness [36,37,39,40]. Under these conditions, trajectory morphology may change substantially across scales. Consequently, a metric emphasizing global morphological similarity, such as the Fréchet distance, may become progressively less sensitive to the physiological reduction in multiscale complexity observed with conventional HFD.

Within this perspective, fractal properties can be interpreted as the multiscale expression of the feedback–synchrony–plasticity (FeeSyCy) principle [7,41,42]. This principle operates across levels of organization, from local neuronal populations to large-scale networks, shaping the temporal structure of neuronal activity [43,44]. In this framework, fractal dimension may reflect the role of neuronal populations within the network. Nodes that are more integrative hubs and functionally closer to such hubs may express richer multiscale temporal dynamics, resulting in higher fractal dimension values. While this interpretation remains indirect, it is consistent with the observed differences across cortical regions and with previous findings linking network organization and signal complexity [45].

Brownian motion and the Weierstrass function represent two models of fractal dynamics that capture stochastic and self-similar forms of scale-invariant complexity, respectively. A stable fractal-dimension estimate across different values of the scale parameter k indicates that the measure accurately captures the intrinsic fractal properties of these models. Notably, HFDf was particularly accurate for the Weierstrass function, suggesting that it is especially sensitive to deterministic self-similar structure. Moreover, unlike the standard HFD, whose estimates for sEEG signals tend to converge toward a value of approximately 2 as K_{max} increases, HFDf reaches a stable asymptotic value below 2. This behavior may represent a step toward the development of more suitable estimators for characterizing the fractality of neurodynamics.

4.4. Local Fluctuations as Expression of Excitation–Inhibition Balance

Balanced excitation and inhibition characterize local and large-scale neuronal networks and support stable yet flexible information processing. Within this regime, neural activity exhibits intrinsic variability, which is not merely noise but a fundamental component of network function. Local fluctuations in neurodynamics can thus be interpreted as the observable manifestation of excitation–inhibition balance operating across scales [45]. These fluctuations contribute to the nonstationary and multiscale properties of neural signals [44] and provide a mechanistic substrate for the fractal features captured by the Higuchi fractal dimension, reflecting the dynamic equilibrium underlying neuronal communication.

4.5. Functional Interpretation Across Primary Cortical Areas

The observed differences in fractal dimension across cortical regions are consistent with their functional roles within sensorimotor processing [46]. Aware that a mechanistic validation would require specific behavioral assessment, we interpret the finding as in agreement with previous findings, where the fractal dimension of M1 activity was higher than that of S1, and both exceeded that of A1. This gradient can be interpreted in light of the functional hierarchy of these areas [47,48]. Motor cortex activity integrates planning, execution, and feedback processes, requiring coordination across multiple levels of control. Such integrative function may be associated with richer multiscale temporal dynamics. Somatosensory processing, while still involving integration, operates at an intermediate level, whereas primary auditory processing may rely on more specialized and temporally constrained dynamics. While this interpretation remains speculative, it is consistent with the idea that the complexity of neurodynamic signals reflects the functional demands and network embedding of the underlying neuronal populations.

4.6. Implications and Future Directions

Overall, these findings refine the interpretation of neurodynamic measures. Fractal dimension provides a robust, structure-sensitive descriptor of regional activity, capable of capturing meaningful differences in ongoing neuronal dynamics.

At the same time, the present results indicate that incorporating morphology-sensitive metrics such as the Fréchet distance into fractal estimation does not straightforwardly

enhance sensitivity for cortical parcellation. This suggests that similarity of temporal trajectories and multiscale complexity capture distinct aspects of neuronal dynamics.

Future work should investigate alternative approaches capable of capturing scale-dependent temporal features of neuronal dynamics, particularly in relation to their physiological and functional relevance. In this perspective, combining multiscale complexity measures with metrics sensitive to local temporal structure may provide a more comprehensive characterization of neurodynamics, with potential implications for neuroimaging-informed neuromodulation strategies.

4.7. Limitations of the Study

The interpretation of the results presented here should account for several limitations. The dataset consists of sEEG recordings from patients with refractory focal epilepsy. The authors of the MNI dataset [28,29] selected channels only from areas clinically spared by the pathology. The MNI dataset offers unique access to intracranial recordings from clinically spared cortical regions, which are not available in healthy individuals for ethical reasons. However, we explicitly acknowledge that the pathological background cannot be fully excluded as a possible influence on local neurodynamics.

A further point concerns the unequal sample sizes available for each cortical pair across wakefulness and sleep stages. The core comparison is M1 versus S1, since these are the cortical regions investigated in the seminal non-invasive study [9] and are especially interesting because, although anatomically contiguous and continuously involved in virtually any behavioral expression, they play distinct neurodynamic roles. The A1 comparisons are retained as exploratory extensions within the available MNI dataset. Finally, even though the selection of a single channel per subject per area was standardized, a single electrode can only offer a 'snapshot' of the local neurodynamics, potentially missing the full spatial variability within each area. Notably, once a neurodynamic measure capable of reliably differentiating cortical regions at the population level is identified, evaluating its stability across alternative channels within the same cortical area will become a crucial validation step. Such analyses would help determine whether the observed regional signatures truly reflect area-specific neurodynamics rather than local sampling variability.

Another limitation of HFDf is its computational load. The computational load of the standard Higuchi fractal dimension estimation is $O(NK_{\max})$, where N is the length of the sequence and $K_{\max}$ is the maximum scale. In the proposed method, the pointwise distance used in HFD is replaced by the discrete Fréchet distance between the original curve and its sub-sampled representation. For a signal of length N, the comparison at scale k involves curves of approximately N and N/k points, resulting in a computational cost of $O(N^2/k)$ per scale. Summing over all scales from 2 to $K_{\max}$, the overall computational complexity becomes $O(N^2 \log K_{\max})$, which is higher than that of the standard HFD algorithm.

5. Conclusions

The present findings suggest that scale-free neurodynamics should not necessarily be interpreted as self-similar neurodynamics. While HFD remains sensitive to the persistence of multiscale organization, introducing a morphology-sensitive metric did not improve discrimination and even attenuated the expected wake–sleep complexity modulation. This observation suggests that the governing principles underlying cortical neurodynamics may persist across scales without requiring preservation of trajectory morphology.

Importantly, these findings underline that self-similarity and scale-free organization should not be considered interchangeable concepts in the nervous system. While self-similarity implies preservation of trajectory morphology across scales, scale-free organization may

instead emerge through recurrent functional relationships among dynamically interacting neuronal populations, even when the corresponding temporal patterns differ in shape.

In this framework, the present results suggest that cortical neurodynamics are not primarily characterized by the recurrence of identical temporal motifs across scales, but rather by the persistence of structured functional relationships among distinct dynamic patterns.

This interpretation may also help explain why entropy-derived measures, despite effectively capturing statistical properties of neural signals, often show limited sensitivity in discriminating local cortical neurodynamics compared with fractal approaches. Indeed, scale-free neurodynamic organization may rely not simply on statistical regularity, but on the coordinated recurrence of functionally related—though not geometrically identical—temporal patterns across structural and functional levels of organization.

In this study, we investigated whether Fréchet distance-based modification of the Higuchi fractal dimension can enhance the distinction between cortical parcels at the intra-subject level, further supporting the concept of region-specific neurodynamic fingerprints. Our results indicate that the proposed modification has similar capability to the standard HFD method for neurodynamics differentiation across cortical areas. However, an important finding is that, unlike the standard HFD, which is strongly dependent on the choice of Kmax, the Fréchet-based estimate converges toward a stable asymptote. This suggests improved robustness of the metric with respect to parameter selection. Overall, these findings contribute to the refining quantitative approaches for analyzing brain dynamics, while reaffirming the reliability of established methods and supporting their application in neurodynamic mapping and neuroimaging-informed neuromodulation strategies.

Supplementary Materials: The following supporting information can be downloaded at https://www.mdpi.com/article/10.3390/fractalfract10070458/s1, Table S1: Extensive information about representative channel selection for different subjects and multiple sEEG channels.

Author Contributions: Conceptualization, F.T. and F.C.; methodology F.T., F.C., K.A. and L.C. (Livio Conti); validation, L.C. (Livio Conti)., C.P., F.T., K.A., F.B., F.M., A.Q. and L.P.; formal analysis, A.P.M.R. and L.C. (Lorenza Cicerone); investigation, F.T., K.A. and L.C. (Livio Conti); resources, F.T.; data curation, K.A., and F.C.; writing—original draft preparation, F.T.; writing—review and editing, A.Q., L.C. (Livio Conti), K.A., C.P., F.B., F.M. and F.T.; visualization, L.C. (Lorenza Cicerone) and A.P.M.R.; supervision, F.T.; project administration, F.T. and F.C. All authors have read and agreed to the published version of the manuscript.

Funding: This research received no external funding.

Institutional Review Board Statement: Ethical review was waived for this study due to the use of pre-existing, de-identified data from the MNI Open iEEG Atlas. The original collection was approved by the IRB of the Montreal Neurological Institute (McGill University).

Informed Consent Statement: Written informed consent was obtained for the original data collection. As this study uses anonymized public data, additional consent was not required.

Data Availability Statement: Data is published by the Montreal Neurological Institute (MNI) at https://mni-open-ieegatlas.research.mcgill.ca/main.php (accessed on 1 May 2026).

Acknowledgments: We thank those who made this dataset publicly available. For English language style and grammar adjustments, we use the Grammarly free version. The authors have reviewed and edited the output and take full responsibility for the content of this publication.

Conflicts of Interest: The authors declare no conflicts of interest.

Abbreviations

The following abbreviations are used in this manuscript:

A1	Primary auditory cortex
FeeSyCy	Feedback–synchrony–plasticity
HFD	Higuchi fractal dimension
HFDf	Higuchi fractal dimension with Fréchet distance
M1	Primary motor cortex
MNI	Montreal Neurological Institute
S1	Primary somatosensory cortex
sEEG	Stereotactic electroencephalography

References

1. Edwards, A.M.; Phillips, R.A.; Watkins, N.W.; Freeman, M.P.; Murphy, E.J.; Afanasyev, V.; Buldyrev, S.V.; da Luz, M.G.; Raposo, E.P.; Stanley, H.E.; et al. Revisiting Lévy flight search patterns of wandering albatrosses, bumblebees and deer. *Nature* **2007**, *449*, 1044–1048. [CrossRef] [PubMed]
2. Beggs, J.M.; Plenz, D. Neuronal Avalanches in Neocortical Circuits. *J. Neurosci.* **2003**, *23*, 11167–11177. [CrossRef] [PubMed]
3. He, B.J.; Zempel, J.M.; Snyder, A.Z.; Raichle, M.E. The temporal structures and functional significance of scale-free brain activity. *Neuron* **2010**, *66*, 353–369. [CrossRef] [PubMed]
4. Eytan, D.; Marom, S. Dynamics and effective topology underlying synchronization in networks of cortical neurons. *J. Neurosci.* **2006**, *26*, 8465–8476. [CrossRef] [PubMed]
5. Expert, P.; Lambiotte, R.; Chialvo, D.R.; Christensen, K.; Jensen, H.J.; Sharp, D.J.; Turkheimer, F. Self-similar correlation function in brain resting-state functional magnetic resonance imaging. *J. R. Soc. Interface* **2011**, *8*, 472–479. [CrossRef] [PubMed]
6. Panksepp, J. Affective consciousness: Core emotional feelings in animals and humans. *Conscious. Cogn.* **2005**, *14*, 30–80. [CrossRef] [PubMed]
7. Tecchio, F.; Bertoli, M.; Gianni, E.; L'Abbate, T.; Paulon, L.; Zappasodi, F. To Be Is To Become. Fractal Neurodynamics of the Body-Brain Control System. *Front. Physiol.* **2020**, *11*, 609768. [CrossRef] [PubMed]
8. Buzsaki, G.; Mizuseki, K. The log-dynamic brain: How skewed distributions affect network operations. *Nat. Rev. Neurosci.* **2014**, *15*, 264–278. [CrossRef] [PubMed]
9. Cottone, C.; Porcaro, C.; Cancelli, A.; Olejarczyk, E.; Salustri, C.; Tecchio, F. Neuronal electrical ongoing activity as a signature of cortical areas. *Brain Struct. Funct.* **2017**, *222*, 2115–2126. [CrossRef] [PubMed]
10. Tecchio, F.; Zappasodi, F.; Pasqualetti, P.; Rossini, P.M. Neural connectivity in hand sensorimotor brain areas: An evaluation by evoked field morphology. *Hum. Brain Mapp.* **2005**, *24*, 99–108. [CrossRef] [PubMed]
11. Tecchio, F.; Pasqualetti, P.; Pizzella, V.; Romani, G.; Rossini, P.M. Morphology of somatosensory evoked fields: Inter-hemispheric similarity as a parameter for physiological and pathological neural connectivity. *Neurosci. Lett.* **2000**, *287*, 203–206. [CrossRef] [PubMed]
12. Pascarella, A.; Bruni, V.; Armonaite, K.; Porcaro, C.; Conti, L.; Cecconi, F.; Paulon, L.; Vitulano, D.; Tecchio, F. Functional balance at rest of hemispheric homologs assessed via normalized compression distance. *Front. Neurosci.* **2024**, *17*, 1261701. [CrossRef] [PubMed]
13. Chialvo, D.R. Emergent complex neural dynamics. *Nat. Phys.* **2010**, *6*, 744–750. [CrossRef]
14. Khazipov, R.; Sirota, A.; Leinekugel, X.; Holmes, G.L.; Ben-Ari, Y.; Buzsáki, G. Early motor activity drives spindle bursts in the developing somatosensory cortex. *Nature* **2004**, *432*, 758–761. [CrossRef] [PubMed]
15. Moaveninejad, S.; Cauzzo, S.; Porcaro, C. Fractal dimension and clinical neurophysiology fusion to gain a deeper brain signal understanding: A systematic review. *Inf. Fusion* **2025**, *118*, 102936. [CrossRef]
16. Olejarczyk, E.; Gotman, J.; Frauscher, B. Region-specific complexity of the intracranial EEG in the sleeping human brain. *Sci. Rep.* **2022**, *12*, 451. [CrossRef] [PubMed]
17. Eiter, T.; Mannila, H. *Computing Discrete Fréchet Distance*; Technical University of Vienna: Vienna, Austria, 1994. Available online: https://www.kr.tuwien.ac.at/staff/eiter/et-archive/files/cdtr9464.pdf (accessed on 1 May 2026).
18. Wylie, T.; Zhu, B. Following a curve with the discrete Fréchet distance. *Theor. Comput. Sci.* **2014**, *556*, 34–44. [CrossRef]
19. Jeremic, A.; Nikolic, D. Detecting Neonatal Seizures using Short Time Fourier Transform and Frechet Distance. In *Proceedings of the 13th International Joint Conference on Biomedical Engineering Systems and Technologies*; SCITEPRESS—Science and Technology Publications: Setúbal, Portugal, 2020; pp. 342–347. [CrossRef]
20. Brakatsoulas, S.; Pfoser, D.; Salas, R.; Wenk, C. On map-matching vehicle tracking data. In *VLDB'05: Proceedings of the 31st International Conference on Very Large Data Bases*; VLDB Endowment: New York, NY, USA, 2005; pp. 853–864.

21. Sriraghavendra, E.; Karthik, K.; Bhattacharyya, C. Fréchet Distance Based Approach for Searching Online Handwritten Documents. In *Ninth International Conference on Document Analysis and Recognition (ICDAR 2007)*; IEEE: Piscataway, NJ, USA, 2007; pp. 461–465. [CrossRef]
22. Cleasby, I.R.; Wakefield, E.D.; Morrissey, B.J.; Bodey, T.W.; Votier, S.C.; Bearhop, S.; Hamer, K.C. Using time-series similarity measures to compare animal movement trajectories in ecology. *Behav. Ecol. Sociobiol.* **2019**, *73*, 151. [CrossRef]
23. Gui, A.; Gamper, H.; Braun, S.; Emmanouilidou, D. Adapting Frechet Audio Distance for Generative Music Evaluation. In *ICASSP 2024—2024 IEEE International Conference on Acoustics, Speech and Signal Processing (ICASSP)*; IEEE: Piscataway, NJ, USA, 2024; pp. 1331–1335. [CrossRef]
24. Tecchio, F.; Cecconi, F.; Colamartino, E.; Padalino, M.; Valci, L.; Reinert, M. The Morphology of Somatosensory Evoked Potentials During Middle Cerebral Artery Aneurysm Clipping (MoSAC): A Pilot Study. *Clin. EEG Neurosci.* **2020**, *51*, 130–136. [CrossRef] [PubMed]
25. Higuchi, T. Approach to an irregular time series on the basis of the fractal theory. *Phys. D* **1988**, *31*, 277–283. [CrossRef]
26. Armonaite, K.; Bertoli, M.; Paulon, L.; Gianni, E.; Balsi, M.; Conti, L.; Tecchio, F. Neuronal Electrical Ongoing Activity as Cortical Areas Signature: An Insight from MNI Intracerebral Recording Atlas. *Cereb. Cortex* **2022**, *32*, 2895–2906. [CrossRef] [PubMed]
27. Armonaite, K.; Nobili, L.; Paulon, L.; Balsi, M.; Conti, L.; Tecchio, F. Local neurodynamics as a signature of cortical areas: New insights from sleep. *Cereb. Cortex* **2022**, *33*, 3284–3292. [CrossRef] [PubMed]
28. Frauscher, B.; Von Ellenrieder, N.; Zelmann, R.; Doležalová, I.; Minotti, L.; Olivier, A.; Hall, J.; Hoffmann, D.; Nguyen, D.K.; Kahane, P.; et al. Atlas of the normal intracranial electroencephalogram: Neurophysiological awake activity in different cortical areas. *Brain* **2018**, *141*, 1130–1144. [CrossRef] [PubMed]
29. von Ellenrieder, N.; Gotman, J.; Zelmann, R.; Rogers, C.; Nguyen, D.K.; Kahane, P.; Dubeau, F.; Frauscher, B. How the Human Brain Sleeps: Direct Cortical Recordings of Normal Brain Activity. *Ann. Neurol.* **2020**, *87*, 289–301. [CrossRef] [PubMed]
30. Alt, H.; Godau, M. Computing the Fréchet distance between two polygonal curves. *Int. J. Comput. Geom. Appl.* **1995**, *5*, 75–91. [CrossRef]
31. Fiel Peres, F. Effect sizes for nonparametric tests. *Biochem. Med.* **2026**, *36*, 010101. [CrossRef] [PubMed]
32. Buzsáki, G.; Logothetis, N.; Singer, W. Scaling Brain Size, Keeping Timing: Evolutionary Preservation of Brain Rhythms. *Neuron* **2013**, *80*, 751–764. [CrossRef] [PubMed]
33. Baertsch, N.A.; Severs, L.J.; Anderson, T.M.; Ramirez, J.-M. A spatially dynamic network underlies the generation of inspiratory behaviors. *Proc. Natl. Acad. Sci. USA* **2019**, *116*, 7493–7502. [CrossRef] [PubMed]
34. Schirner, M.; Deco, G.; Ritter, P. Learning how network structure shapes decision-making for bio-inspired computing. *Nat. Commun.* **2023**, *14*, 2963. [CrossRef] [PubMed]
35. Liaw, S.-S.; Chen, J.-Y. Characterizing Sleep Stages by the Fractal Dimensions of Electroencephalograms. *Biostat. Biom. Open Acc. J.* **2017**, *2*, 555584. [CrossRef]
36. Spoormaker, V.I.; Czisch, M.; Maquet, P.; Jäncke, L. Large-scale functional brain networks in human non-rapid eye movement sleep: Insights from combined electroencephalographic/functional magnetic resonance imaging studies. *Philos. Trans. R. Soc. A Math. Phys. Eng. Sci.* **2011**, *369*, 3708–3729. [CrossRef] [PubMed]
37. Wehrle, R.; Kaufmann, C.; Wetter, T.C.; Holsboer, F.; Auer, D.P.; Pollmächer, T.; Czisch, M. Functional microstates within human REM sleep: First evidence from fMRI of a thalamocortical network specific for phasic REM periods. *Eur. J. Neurosci.* **2007**, *25*, 863–871. [CrossRef] [PubMed]
38. Moruzzi, G. The sleep-waking cycle. *Ergeb. Physiol.* **1972**, *64*, 1–165. [CrossRef]
39. Parrino, L.; Vaudano, A.E. The resilient brain and the guardians of sleep: New perspectives on old assumptions. *Sleep Med. Rev.* **2018**, *39*, 98–107. [CrossRef] [PubMed]
40. Ameen, M.S.; Jacobs, J.; Schabus, M.; Hoedlmoser, K.; Donoghue, T. Temporally resolved analyses of aperiodic features track neural dynamics during sleep. *Commun. Psychol.* **2025**, *3*, 160. [CrossRef] [PubMed]
41. Grossberg, S. Adaptive Resonance Theory: How a brain learns to consciously attend, learn, and recognize a changing world. *Neural Netw.* **2013**, *37*, 1–47. [CrossRef] [PubMed]
42. Francis, M.; Markus, A.; Stuhr-Wulff, F.; Shamay-Tsoory, S. Shaping inter-brain plasticity: A feasibility study of enhancing inter-brain synchrony with dyadic neurofeedback. *iScience* **2026**, *29*, 114894. [CrossRef] [PubMed]
43. Turrigiano, G.G.; Nelson, S.B. Homeostatic plasticity in the developing nervous system. *Nat. Rev. Neurosci.* **2004**, *5*, 97–107. [CrossRef] [PubMed]
44. Cross, Z.R.; Gray, S.M.; Dede, A.J.; Rivera, Y.M.; Yin, Q.; Vahidi, P.; Rau, E.M.; Cyr, C.; Holubecki, A.M.; Asano, E.; et al. The development of aperiodic neural activity in the human brain. *Nat. Hum. Behav.* **2025**, *9*, 2548–2563. [CrossRef] [PubMed]
45. Bassett, D.S.; Siebenhühner, F. Multiscale Network Organization in the Human Brain. In *Multiscale Analysis and Nonlinear Dynamics*; Wiley: Hoboken, NJ, USA, 2013; pp. 179–204. [CrossRef]
46. Stam, C.J.; Reijneveld, J.C. Graph theoretical analysis of complex networks in the brain. *Nonlinear Biomed. Phys.* **2007**, *1*, 3. [CrossRef] [PubMed]

47. Friston, K. Hierarchical Models in the Brain. *PLoS Comput. Biol.* **2008**, *4*, e1000211. [CrossRef] [PubMed]
48. Paquola, C.; Vos De Wael, R.; Wagstyl, K.; Bethlehem, R.A.; Hong, S.J.; Seidlitz, J.; Bullmore, E.T.; Evans, A.C.; Misic, B.; Margulies, D.S.; et al. Microstructural and functional gradients are increasingly dissociated in transmodal cortices. *PLoS Biol.* **2019**, *17*, e3000284. [CrossRef] [PubMed]